Journal of Theoretical Biology 291 (2011) 33–41

Contents lists available at SciVerse ScienceDirect

Journal of Theoretical Biology

journal homepage: www.elsevier.com/locate/yjtbi

# Modeling oxygen transport in human placental terminal villi

J.S. Gill [a,*], C.M. Salafia [b], D. Grebenkov [c], D.D. Vvedensky [a]

[a] The Blackett Laboratory, Imperial College London, London SW7 2AZ, United Kingdom
[b] Placental Analytics LLC, 93 Colonial Avenue, Larchmont, NY 10538, United States
[c] LPMC, CNRS – Ecole Polytechnique, F-91128 Palaiseau, France

ARTICLE INFO

*Article history:*
Received 3 June 2011
Received in revised form
12 September 2011
Accepted 13 September 2011
Available online 22 September 2011

*Keywords:*
Placental transport
Diffusion equation
Diffusional screening
Transport efficiency

ABSTRACT

Oxygen transport from maternal blood to fetal blood is a primary function of the placenta. Quantifying the effectiveness of this exchange remains key in identifying healthy placentas because of the great variability in capillary number, caliber and position within the villus—even in placentas deemed clinically "normal". By considering villous membrane to capillary membrane transport, stationary oxygen diffusion can be numerically solved in terminal villi represented by digital photomicrographs. We aim to provide a method to determine whether and if so to what extent diffusional screening may operate in placental villi.

Segmented digital photomicrographs of terminal villi from the Pregnancy, Infection and Nutrition study in North Carolina 2002 are used as a geometric basis for solving the stationary diffusion equation. Constant maternal villous oxygen concentration and perfect fetal capillary membrane absorption are assumed. System efficiency is defined as the ratio of oxygen flux into a villus and the sum of the capillary areas contained within. Diffusion screening is quantified by comparing numerical and theoretical maximum oxygen fluxes.

A strong link between various measures of villous oxygen transport efficiency and the number of capillaries within a villus is established. The strength of diffusional screening is also related to the number of capillaries within a villus.

Our measures of diffusional efficiency are shown to decrease as a function of the number of capillaries per villus. This low efficiency, high capillary number relationship supports our hypothesis that diffusional screening is present in this system. Oxygen transport per capillary is reduced when multiple capillaries compete for diffusing oxygen. A complete picture of oxygen fluxes, capillary and villus areas is obtainable and presents an opportunity for future work.



## 1. Introduction

The placenta is the sole source of oxygen and nutrients for the fetus, with adequate oxygenation essential for fetal growth. Placental transport function is one of the main factors in the health and development of both the fetus and the placenta itself. The fetal origins of adult health hypothesis (Barker, 1995) suggest that placental development is even linked to adult health—the effects of oxygen transport on placental growth and function are clearly important. Although oxygen uptake does not completely describe the system, transport characteristics can be a good proxy for placental development (Lackman et al., 2001). Due to the complex structure of the system, a full quantitative analysis of oxygen transport is difficult to obtain *in vivo* but numerical models can potentially provide suitable substitutes.

The placenta grows and develops alongside the fetus and is almost completely fetally genetic. The mature placenta is often disk-shaped with a radius of around 9.5 cm and thickness of 2.5 cm, but there are also large variations in morphology (Gill et al., 2011). The surface of the placenta attached to the endometrium (lining) of the uterine wall is called the basal plate and the surface nearest the fetus the chorionic plate (Fig. 1). Between the two is a complex arborised vascular network through which oxygen, nutrient and waste exchange takes place. The umbilical cord contains two arteries and one vein from the fetus and connects to the placenta on the chorionic plate. At the chorionic surface the blood vessels branch across the surface of the placenta before diving down into the tissue. The vascular network branches progressively from the chorionic plate creating a complex system of villi which terminate in "terminal villi" which contains a branched system of capillary loops. The whole vascular tree is enclosed within a structural tissue matrix (stroma) and a membrane—the villous membrane. The smallest branches of the villous tree are called terminal villi, and it is here where the

* Corresponding author.
*E-mail address:* joshua.gill@imperial.ac.uk (J.S. Gill).

0022-5193/$ - see front matter © 2011 Elsevier Ltd. All rights reserved.
doi:10.1016/j.jtbi.2011.09.008

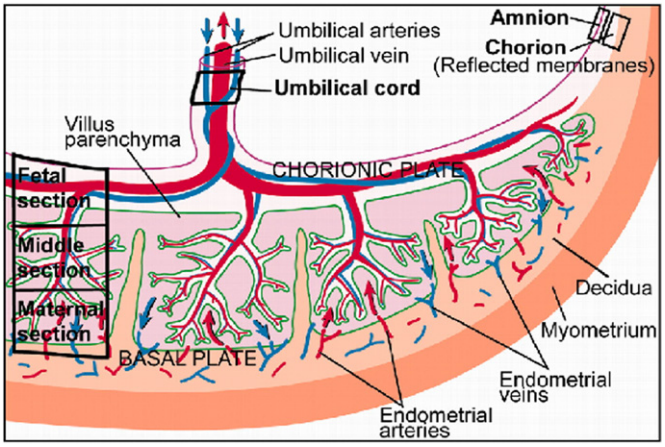


**Fig. 1.** Schematic view of the placenta showing the chorionic plate, the basal plate and the branching vascular system of the placenta. Reproduced with permission from R. Sood, J. L. Zehnder, M. L. Druzin, and P. O. Brown, Proc. Natl. Acad. Sci. USA, 103(14), 5478 (2006). Copyright (2006) National Academy of Sciences, USA.

villous membrane is thinnest and consequently where oxygen is transferred. Surrounding the villous tree is a connected region called the intervillous space through which maternal blood flows. The capillaries of the terminal villi are the site of oxygen and nutrient transfer between the maternal and fetal bloodstreams. Injection studies have confirmed that these terminal channels are exclusively capillaries rather than lymphatic or other types of inter-cellular channels (Castellucci and Kaufmann, 1982; Kaufmann et al., 1985; Lee and Yeh, 1986, 1983).

The process of oxygen transfer from maternal to fetal blood can be broken down into three stages.

(i) Oxygenated maternal blood enters the placenta through 100–150 spiral arteries located in the basal plate (Boyd and Hamilton, 1970) and fills the intervillous space. The villi themselves are geometric obstacles to blood flow, so flow rates decrease from the basal to chorionic plates. Consequently different individual villi are subject to different maternal oxygen concentrations.

(ii) Once oxygenated blood reaches a terminal villus, oxygen diffuses across the villous membrane and stroma to the fetal capillaries. This diffusive flow arises due to the concentration gradient between the villous membrane (high oxygen concentration) and the fetal capillary membrane (low oxygen concentration).

(iii) Finally, oxygenated fetal blood is transferred via the fetal vascular network (described above) to the fetus.

The fetal placental capillary network is extremely complex and also highly variable, not only between placentas but within the same placenta. A number of maternal and fetal conditions have been associated with changes in the number, caliber and position of capillaries within terminal villi. Preterm preeclampsia associated with maternal uteroplacental vascular pathology often yield terminal villi with non-branching angiogenesis, seen as simple and small villi with few capillaries (Benirschke et al., 2006a). Disorders such as maternal diabetes and anemia, as well as high altitude exposure, are each associated with the converse, namely extensive branching angiogenesis which is represented in 2-D cross sections as many capillary lumens, often located centrally within the villus and remote to the maternal intervillous flow. In either situation, the fetus may be at risk, whether for preterm birth, abnormally small or large size, or intolerance of labor (Benirschke et al., 2006a).

Placentas with too few villi and too few vessels in those villi may simply fail to transport enough oxygen to support the fetus. Such placentas may also pose an increased burden to the fetal heart, with increased placental vascular resistance due to the reduced capillary bed. Villi with too many or too tortuous vessels are also recognized as pathological, termed "chorangiosis" or "chorangiomatosis" (Ogino and Redline, 2000).

The functional significance of the histologic categorization of "too few" or "too many" villi is not known, mainly because of the difficulty in understanding the complex effects of capillary number, caliber, and location on placental capillary function. Understanding the spectrum of functional efficiency of the broad range of villous capillary geometries in a term placenta would be a first step to a categorization. Once a range of functional efficiencies is established, one could begin to test at what level(s) the label "pathological" might be applied, in both fetal (e.g. abnormal fetal growth) and maternal (e.g. preeclampsia and maternal diabetes) contexts. Given the current state of knowledge, it is therefore not surprising that the mechanism(s) by which such capillary abnormalities cause the clinical outcomes is unclear (Amer and Heller, 2010). It also unknown whether the capillary abnormalities are simply correlated with, rather than causal to, those outcomes.

One mechanism could be an increased fetal cardiac workload due to the increased size of the placental capillary bed. However, there should be benefits from increased capillary number in terms of oxygen extraction from the maternal intervillous bloodstream. Such benefits could be limited either if the cardiac workload imposed was greater than the increased amount of oxygen extracted could provide, or if structural effects reduced the efficiency of the villus as a whole by reducing the efficiency of capillaries forced to "compete" with each other for diffusing oxygen.

Such a mechanism has been well described in the lung (Felici et al., 2003; Grebenkov et al., 2005; Felici et al., 2005). In that organ, diffusional screening is thought to be the basis for pulmonary functional reserve; i.e., while diffusional screening operates at rest, in exercise increased respiratory rates create a more uniform alveolar gas, reducing the effects of acinar geometry on alveolar oxygen tension, and eliminating diffusional screening. In the placenta, diffusional screening may be more problematic, as the "resting" placenta normally receives 40–50% of fetal cardiac output, and normal maternal intervillous flows are $\sim$700–1000 ml/min. Thus the normal placenta more closely resembles an exercising lung. Extra capillaries may be as problematic as "missing" capillaries, damaged by abnormal maternal blood flow (Burton et al., 2009).

Previous work has modeled maternal–fetal oxygen transfer in a number of ways. Terminal villus oxygen transfer has been approximated as a shunted placental 'exchange unit' including an equation for oxygen concentration of blood (Kirschbaym and Shapiro, 1969). Costa et al. treated the placenta as a collection of capillaries exchanging oxygen as 'flat walls' (i.e., one-dimensional transfer). Their work takes account of capillary structure such as sinusoids (Costa et al., 1992). Additionally, a number of papers used ordinary differential equations across the whole diffusion surface, both time-dependent (Hill et al., 1973) and time-independent (Lardner, 1975).

The bulk of prior work that models maternal–fetal oxygen transfer at the terminal villus stage does so effectively at one interface. In doing so, these models use ordinary differential equations without spatial resolution and thus neglect the complexity of the villus–capillary geometry. Our work differs in that we use partial differential equations to study the spatial dependence of the transport system. Utilizing actual villous shapes as a basis for simulating oxygen transport in specific locations allows us to investigate the effects of the complex geometry upon diffusion.

Calculation of oxygen diffusion in actual terminal villous geometries is undertaken via digital photomicrographs (Fig. 2).

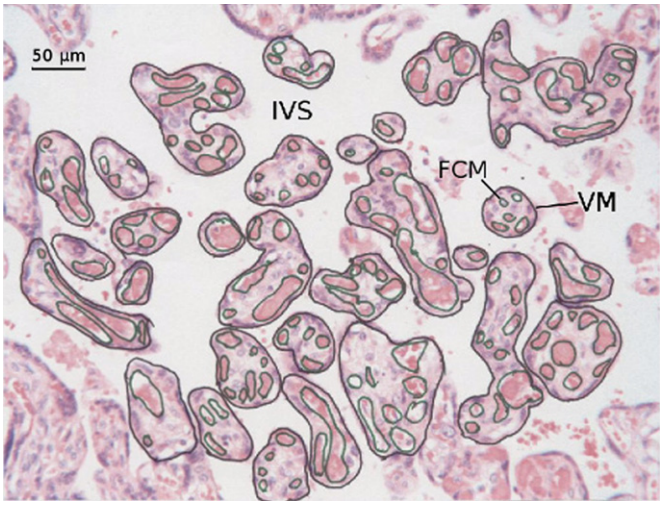


**Fig. 2.** A small fragment of a segmented digital photomicrograph of terminal villi. Maternal blood flows in the intervillous space (IVS) and oxygen is transported from the villous membrane (VM) to the fetal capillary membrane (FCM).

Quantitative values for oxygen fluxes, capillary and villus numbers and areas are obtainable.

Diffusion distances for oxygen transport in terminal villi have also been the subject of past research (Mayhew et al., 1984, 1986). A common way of describing diffusion distances is to calculate the harmonic mean of various membrane thicknesses (Weibel, 1970). This work aims to extend the idea of diffusion distance to a full numerical calculation of diffusion within the geometries of terminal villi. Hence the quantitative effect of various biological diffusion distances in the villi will be easily and visibly understood in terms of their effect on oxygen transport. Harmonic mean distances can still be calculated, but the contribution to oxygen transport from every segmented villus means that a more complete picture can be found. We add to this field the evaluation of the effects of diffusional screening, which has not been examined in this system.

## 2. Materials and methods

### 2.1. Diffusion model

The fetal vascular system is constantly moving oxygenated blood away from the sites of oxygen transfer, so the fetal capillary membrane can be thought of as an oxygen 'sink'. The transfer of oxygen from the villous membrane to the fetal capillary membrane is driven by the concentration gradient between highly oxygenated maternal blood and low oxygenated fetal blood. This is expressed mathematically by Fick's law:

$$\mathbf{J} = -D\nabla c. \tag{1}$$

which states that the amount of oxygen per unit time per unit area, or flux ($\mathbf{J}$), is proportional to the gradient of oxygen concentration inside the villus, $c(x,t)$, with the diffusion coefficient $D$ of oxygen in plasma.

The mass conservation of diffusing oxygen is expressed through the continuity equation:

$$\nabla \cdot \mathbf{J} + \frac{\partial c}{\partial t} = 0. \tag{2}$$

This equation formalises the notion that the rate of change of oxygen (with time) in a region is balanced by the amount of oxygen entering or leaving that region. The continuity equation and Fick's law can be combined to give the diffusion equation:

$$\frac{\partial c}{\partial t} = D\nabla^2 c. \tag{3}$$

The maternal intervillous flow is essentially a large lake of blood with little or no impedance to blood flow (Burton et al., 2009). Placental intervillous blood flow estimates range from 500 ml/min (80% of the uterine perfusion) to approximately 700–1000 ml/min (Burton et al., 2009). Despite this massive blood flow, blood pressure in the intervillous space is only about 6–10 mmHg in the relaxed term uterus (Boyd and Hamilton, 1970). A massive increase in blood flow occurring in the context of a drop in local blood pressure is likely to be related to low resistance, significantly lower than in the systemic circulation.

The oxygen concentration on the terminal villous boundary varies with time due to the pulses of maternal blood from spiral arteries. Comparing the time for maternal blood to travel through the intervillous space (10–20 s) with the time for oxygen to diffuse across a villus (of the order of seconds Burton et al., 2009), this time-dependence can be neglected in a first approximation. Thus in the stationary (time-independent) regime:

$$\nabla^2 c = 0. \tag{4}$$

We have also assumed that the maternal blood oxygen concentration surrounding the terminal villi is a constant, denoted $c_m$. In reality the maternal oxygen concentration is a function of both the position of the terminal villus in the intervillous space and the proximity of other terminal villi.

While the villous tree has many branches, the appearance of density in the delivered placenta is misleading since the intervillous blood space is normally approximately just under twice the depth of the delivered placenta (in vivo 37.5 mm at 35 weeks, Mital et al., 2002, compared to 24 mm at 35 weeks post-partum, Benirschke et al., 2006b). Thus the "density" of villi in the intervillous space as examined histologically post-partum must be recognized as a significant overestimate of the density in the in vivo placenta. The effect of other nearby villi upon the constant maternal oxygen concentration assumption is therefore smaller than that would be expected from the digital photomicrographs alone. Future work aims to investigate the effect of these factors on oxygen concentration at the villous membrane.

The second boundary condition – that on the capillary membrane – is also simplified to a constant oxygen concentration value of $c_f$. This implies that fetal capillaries act as perfect oxygen sinks, further work could include a more realistic finite oxygen permeability (Felici et al., 2003; Grebenkov et al., 2005; Felici et al., 2005). Normalizing the maternal oxygen concentration at the villous membrane to one:

$$u(x,t) = \frac{c(x,t) - c_f}{c_m - c_f},$$

without loss of generality the equations simplify to become:

$$\nabla^2 u = 0,$$

$$u_v = 1,$$

$$u_f = 0.$$

In our simplified model, all fetal capillaries are treated as carrying arterial deoxygenated blood and thus acting as perfect sinks for oxygen, as it is impossible to know from the 2D slice geometry which capillaries carry blood that was oxygenated elsewhere in the villous tree.

The images data for this work were collected as part of a well described birth cohort, the Pregnancy, Infection and Nutrition Study—a study of women recruited at mid-pregnancy from an academic health center in central North Carolina. The study population and

recruitment techniques are described in detail elsewhere (Salafia et al., 2005). Beginning in March 2002, all women recruited into this study were requested to consent to a detailed placental examination. Placental gross examinations, histology reviews, and image analyses were performed at EarlyPath Clinical and Research Diagnostics, a New York State-licensed histopathology facility under the direct supervision of Dr. Carolyn Salafia. Placentas were shipped fixed in a volume of 10% buffered formalin appropriate to their weight. Samples were taken perpendicular to the chorionic and basal plates and dehydrated and embedded in paraffin prior to preparation with routine hematoxylin and eosin stains. We recognize that such preparation yields results that differ markedly from Epon embedding, a histological gold standard (Sen et al., 1979). However, our goal was to develop standards that could be utilized in clinical service. The consistent use of paraffin embedding makes all samples in the present effort comparable. The institutional review board from the University of North Carolina at Chapel Hill approved this protocol.

The image sites were selected from non-marginal samples of non-lesional placental parenchyma; areas of infarct, chronic villitis, or fetal vascular pathology were excluded. The regions of villi analyzed were taken from carefully oriented tissue samples at the midposition between chorionic and basal plates near the edge of the central cavity found in many placental functional units. Here maternal flow is considered to be most uniform and optimal for transport (Benirschke et al., 2006c). Furthermore, the uniform sampling at this level allows the best control, which may yet be imperfect, to compensate for the fact that villi located in different positions within the intervillous space are subjected to maternal blood of different oxygen concentrations. Villus and capillary boundaries were identified by eye and manually traced, with capillaries identified as a single layer of endothelial cells without smooth muscle. Segmented images were loaded into a custom Matlab algorithm.

We used a simple four-point stencil (Fig. 3) so that the oxygen concentration in one pixel depends upon the concentrations in the four nearest-neighbours ($u_{i-1,j}$, $u_{i+1,j}$, $u_{i,j-1}$ and $u_{i,j+1}$). In each iteration the oxygen concentration of a pixel is given by:

$$u_{ij} = (1-\alpha)u_{ij} + \tfrac{1}{4}\alpha(u_{i+1,j} + u_{i-1,j} + u_{i,j+1} + u_{i,j-1}) \quad (5)$$

($\alpha$ is the relaxation parameter used to accelerate convergence of the simulation).

To solve stationary diffusion the pixel values are calculated by successive-over-relaxation (Jaluria and Torrance, 2002) until a stationary solution is found (defined as the point where oxygen flux does not change by more than 1% per iteration). One digital photomicrograph typically takes 10 000 iterations in less than 1 min.

With known oxygen concentrations in the intravillous space, oxygen fluxes into the fetal capillary system can be calculated—hereafter called non-isolated capillary flux. We approximate the oxygen flux to each capillary by summing the oxygen concentrations of the nearest pixels (at distance $a$) to the boundary and then dividing the sum by $a$.

Fig. 4 shows a manually segmented digitized histology slide alongside the simulated intravillous oxygen concentration. Each intravillous pixel of the image represents a grid point to which an oxygen concentration value is initially assigned. The oxygen concentration of pixels representing the membranes is calculated from the boundary conditions.

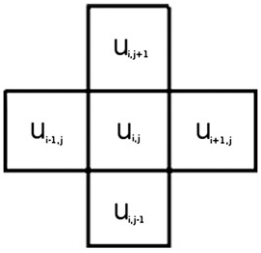


**Fig. 3.** The simple four-point stencil used to calculate oxygen concentration in pixel $i,j$ at each iteration.

### 2.2. Diffusional screening

One of the main objectives of this work is to identify the extent of diffusional screening within terminal villi. Diffusional screening in this context is the phenomenon whereby some capillaries are "shielded" from receiving oxygen by the others. Peripheral fetal capillaries are close to the villous membrane and thus oxygenated maternal blood—they are exposed to a high oxygen concentration gradient and absorb a large amount of oxygen. The oxygen concentration surrounding fetal capillaries situated behind these peripheral vessels is subsequently lower and the central capillaries absorb less oxygen. Peripheral capillaries can be described as screening the more central ones.

Diffusional screening can be quantified by comparing the non-isolated capillary flux for each capillary with the flux of that capillary if the other capillaries were not present (the so-called "isolated capillary" flux). The ratio of these fluxes (denoted $\eta$) provides an indication of how the locations of capillaries influence the oxygen fluxes of others. A value of $\eta = 1$ implies no screening (if the isolated capillary flux and the non-isolated capillary flux are equal then the non-isolated capillary flux can have only arisen from a single-capillary villus) and $\eta = 0$ implies total diffusional screening, i.e., the oxygen flux reaching this capillary is zero due to the shielding effect of other capillaries in the villus.

**Fig. 4.** An example of a segmented histology slide, the membrane boundaries and resulting simulated oxygen concentration. In the right panel, darker shading represents higher oxygen concentration.

### 2.3. Diffusional efficiency

Another method to quantify diffusional transport is to consider some oxygen transport efficiency. An efficiency can be defined as the ratio of some revenue to some cost of the system. In the case of terminal villi, 'revenue' is oxygen flux, while 'cost' can be related to capillary cross-sectional area, simply because larger capillaries require more energy to grow. One way to define the efficiency of a villus containing $N$ capillaries is

$$E_q = \frac{\sum_{n=1}^{N} J_n}{\sum_{n=1}^{N} (A_n)^q} \tag{6}$$

where $J_n$ and $A_n$ are the oxygen flux and area of $n$th capillary, and $q$ is a real parameter. Three specific values of $q$ may have a physical interpretation. For $q=0$, the denominator is simply $N$ and $E_0$ is the average flux per capillary. When $q=1$, the denominator is the total area of capillaries. For $q=2$, capillary area squared (i.e., the fourth power of the capillary radius) is inversely proportional to hemodynamic resistance so that the denominator represents the inverse of the total hemodynamic resistance of capillaries (connected in parallel).

An alternative way to quantify efficiency is the average capillary flux to area ratio

$$\overline{E}_q = \frac{1}{N} \sum_{n=1}^{N} \frac{J_n}{(A_n)^q}. \tag{7}$$

In addition to capillary efficiency, we have also quantified villous structure. With the segmented digital photomicrographs, it is possible to automatically calculate capillary and villus cross-sectional areas and perimeters. This geometric data could be used to potentially highlight abnormal terminal villous structures. We also measure the shortest distance from each capillary membrane to the villous membrane and take the harmonic mean per villus.

## 3. Results and discussion

### 3.1. Quantifying diffusional screening

Non-isolated capillary oxygen fluxes were calculated from a total of 45 digital photomicrographs from 13 placentas. To illustrate the notion of diffusional screening, we present a schematic of a single villus. Fig. 5 shows an example villus containing three capillaries alongside corresponding single-capillary villus arrangements. These representations of the villus are used to calculate isolated capillary fluxes. Non-isolated and isolated capillary fluxes are given in Table 1. The ratio of non-isolated and isolated capillary fluxes ($\eta$) is our measure of diffusional screening. A clear indicator that screening effects result in lower total oxygen flux is that isolated capillary oxygen fluxes are always higher than the non-isolated capillary fluxes calculated with all capillaries present.

The position of capillary 2 in Fig. 5 suggests that it would be somewhat "shielded" from oxygen by the other two capillaries—this is confirmed in Table 1 with the lowest value of $\eta$ of the three capillaries. The lower oxygen flux of capillary 2 is also due in part to its distance from the villus boundary. However, the dependence of the flux on distance is logarithmically weak (see Appendix A), and less significant than any reductions in flux due to screening.


**Fig. 5.** A segmented villus containing three capillaries and the associated images from which "isolated capillary" fluxes are calculated.

**Table 1**
Non-isolated and isolated capillary oxygen fluxes for the capillaries in Fig. 5. Theoretical fluxes are computed using conformal mapping techniques described in Appendix A.

| Capillary | Isolated capillary flux $(\mu m\ s)^{-1}$ | Non-isolated capillary flux, $(\mu m\ s)^{-1}$ | Screening factor, $\eta$ | Theoretical flux $(\mu m\ s)^{-1}$ |
|---|---|---|---|---|
| 1 | 12.87 | 12.27 | 0.95 | 12.50 |
| 2 | 5.03 | 3.35 | 0.67 | 4.76 |
| 3 | 11.54 | 10.31 | 0.89 | 10.96 |


**Fig. 6.** A segmented villus containing five capillaries.

**Table 2**
Non-isolated and isolated capillary oxygen fluxes for the capillaries in Fig. 6.

| Capillary | Isolated capillary flux $(\mu m\ s)^{-1}$ | Non-isolated capillary flux $(\mu m\ s)^{-1}$ | Screening factor, $\eta$ | Theoretical flux $(\mu m\ s)^{-1}$ |
|---|---|---|---|---|
| 1 | 14.59 | 11.95 | 0.82 | 14.61 |
| 2 | 16.38 | 13.67 | 0.83 | 11.73 |
| 3 | 33.71 | 31.03 | 0.92 | 24.30 |
| 4 | 3.98 | 0.03 | 0.01 | 3.89 |
| 5 | 9.24 | 6.31 | 0.68 | 9.09 |

Fig. 6 shows another villus, this time containing five capillaries. The middle capillary, 4, is significantly screened by the surrounding capillaries, with a corresponding screening factor $\eta$ very close to zero. The larger number of capillaries in this villus contributes to lower screening factors for all capillaries compared with Fig. 5.

The final column of Tables 1 and 2 is a theoretical flux. This is the oxygen flux calculated using a conformal mapping technique (detailed in Appendix A) that approximates single-capillary villi to concentric circles allowing analytical fluxes to be found. Table 1 shows how good an approximation by the conformal map can be for circular capillaries and villi—with good agreement between theoretical flux and isolated capillary flux. However, the conformal mapping approach is less suitable for non-circular capillaries, as shown by capillary 3 in Fig. 6. This non-circular capillary has quite different theoretical and isolated capillary fluxes.

### 3.2. Diffusion transport efficiency

As expected our measures of oxygen transport efficiency, $E_1$, $E_2$ and $\overline{E}_1$, strongly depend on the number of capillaries per villus. Once non-isolated capillary fluxes were calculated for all villi, efficiencies were evaluated and plotted as a distribution (Fig. 7). In the top panel, total frequency is plotted vs efficiency, with the histogram bars divided into categories based on the number of capillaries per villus. In the lower panel the $y$-axis is the percentage of each bin in each capillary per villus category. Fig. 7 clearly shows that a larger proportion of 'low-efficiency' villi contain a higher number of capillaries. As a larger number of

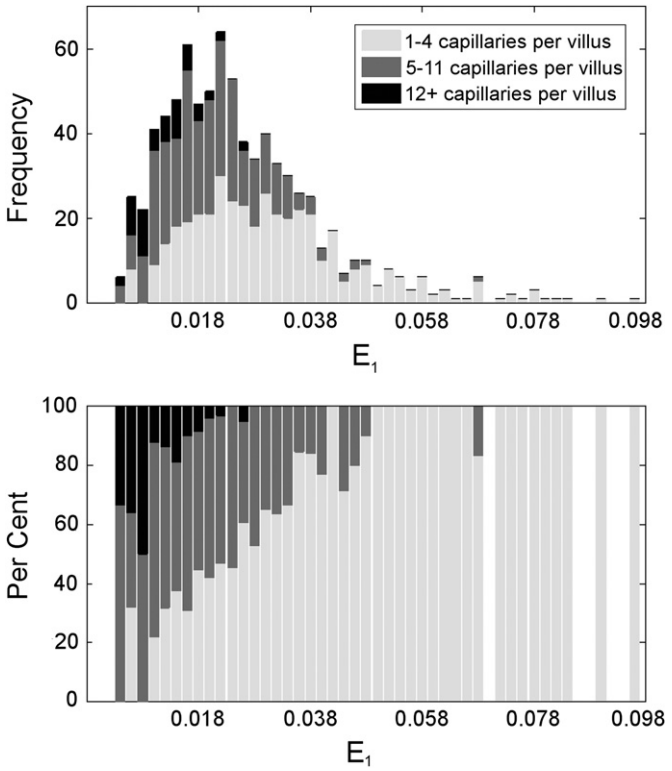


**Fig. 7.** A distribution of oxygen transport efficiency $E_1$. The bars of the histogram show each 'binned' efficiency broken down by number of capillaries per villus. The top panel shows frequency and the bottom percentage.

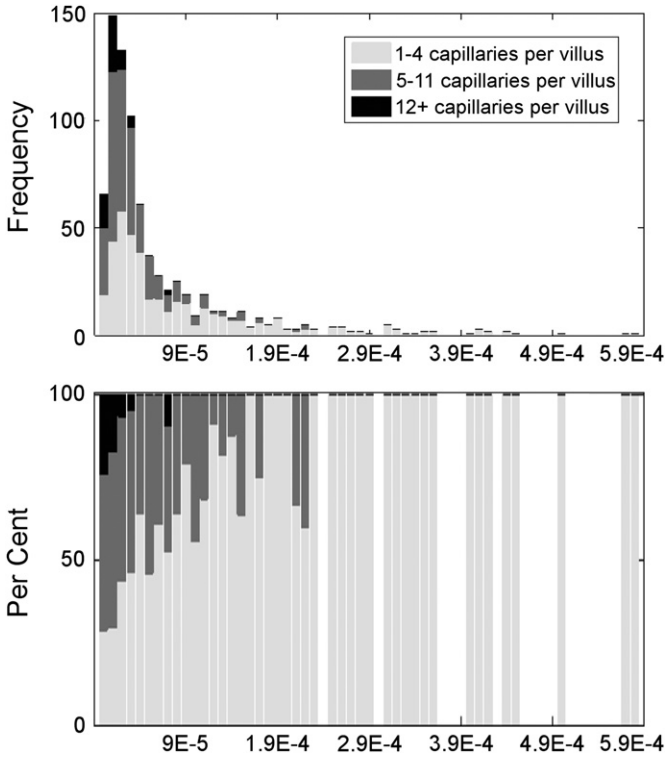


**Fig. 8.** A distribution of oxygen transport efficiency $E_2$. The bars of the histogram show each 'binned' efficiency broken down by number of capillaries per villus. The top panel shows frequency and the bottom percentage.

capillaries within a given villus would lead to stronger diffusional screening, this would seem to confirm that diffusional screening results in lower efficiency, at least by this measure.

Considering efficiency to be the ratio of the sum of oxygen flux and the sum of capillary area squared ($E_2 - q=2$ in Eq. (6)), similar distributions are obtained (Fig. 8). However, in this case the skewed position of villi containing more than four capillaries in the distribution is accentuated. Accumulated areas from multiple capillaries causes a larger effect on the efficiency ratio when squared. The main conclusion is unchanged, however, that low efficiency villi are more likely to contain many capillaries.

Fig. 9 shows how the capillary–villi arrangements can vary significantly even within a single photomicrograph. Two of the labelled villi, A and B, have very low efficiencies (bottom decile) and two, C and D, have a high (top decile) efficiency ($E_1$).

Fig. 10 shows efficiency by the second measure, $\overline{E}_1$ (average capillary efficiency per villus). Again a larger proportion of low efficiency villi are from villi with more capillaries, implying a higher degree of screening.

The measures $E_1$ and $\overline{E}_1$ quantify efficiency in broadly the same way—the ratio of some revenue to some cost (in this case flux and capillary area). Consequently it would be expected that the two measures are correlated. This is confirmed in Fig. 11. Note that $E_1$ and $\overline{E}_1$ reduce to the same quantity when a villus contains one capillary, $E_1 = J_1/A_1$, resulting in the straight line in Fig. 11.

To confirm that both $E_1$ and $\overline{E}_1$ are functions of the number of capillaries per villus, the average efficiency over all villi as a function of the number of capillaries was calculated. The results are shown in Fig. 12. Efficiency clearly decreases as the number of capillaries per villus increases, and seems to follow a power-law. The $E_1$ data has an exponent of $-0.40$ and the exponent of the $\overline{E}_1$ data is $-0.34$.

In our dataset of 13 placentas, 45 digital photomicrographs, there are $4.75 \pm 5.07$ capillaries per villus covering $25.6\% \pm 14.0\%$

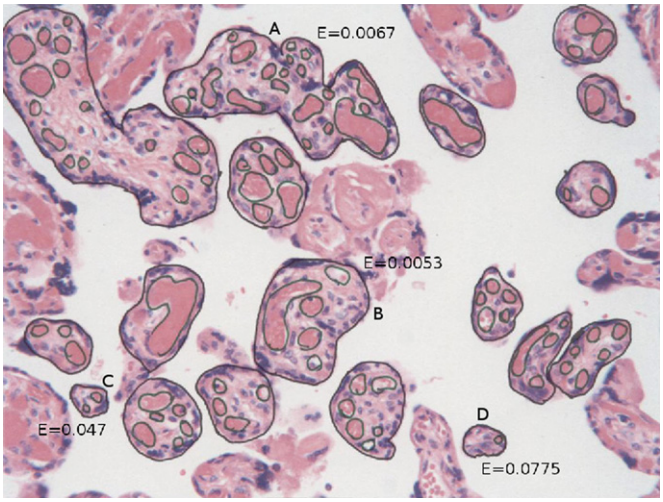


**Fig. 9.** A photomicrograph showing the variation in capillary arrangements. A and B have low efficiencies (bottom decile) and C and D have high efficiencies (top decile). The values for $E_1$ for A, B, C and D are 0.0067, 0.0053, 0.047 and 0.0775 respectively.

of the villus cross-section (mean $\pm$ standard deviation). The mean villus perimeter and area are $359 \pm 264$ μm and $11\,300 \pm 16\,900$ μm$^2$ respectively. Mean capillary perimeter and area are $77.9 \pm 47.1$ μm and $599 \pm 702$ μm$^2$. The harmonic mean of the shortest capillary–villus distance is calculated per villus and the average over all villi is $4.47 \pm 3.69$ μm. This result is in agreement with that obtained via stereological methods (Mayhew et al., 1984).

An advantage of this digital numerical method is that high efficiency and low efficiency villi can be easily found. The panels below (Figs. 13 and 14) show the geometry of some high (within

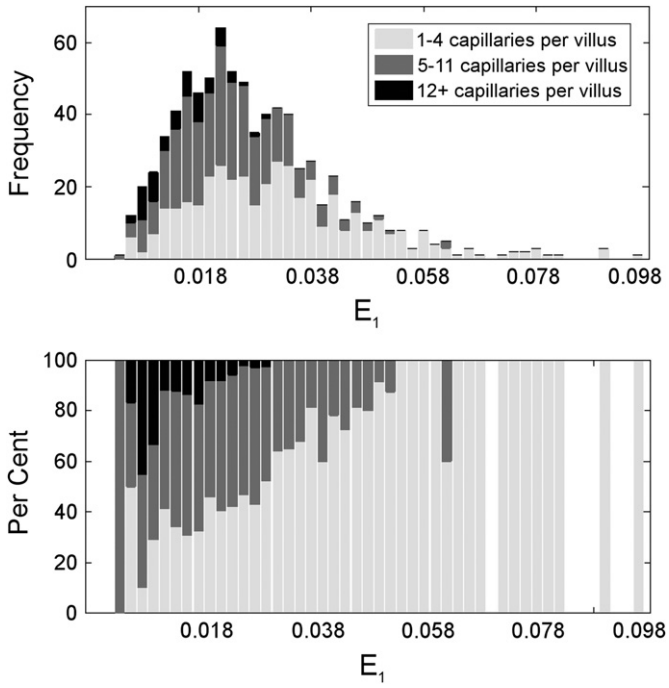


**Fig. 10.** A distribution of oxygen transport efficiency $\bar{E}_1$. The bars of the histogram show each 'binned' efficiency broken down by number of capillaries per villus. The top panel shows frequency and the bottom percentage.

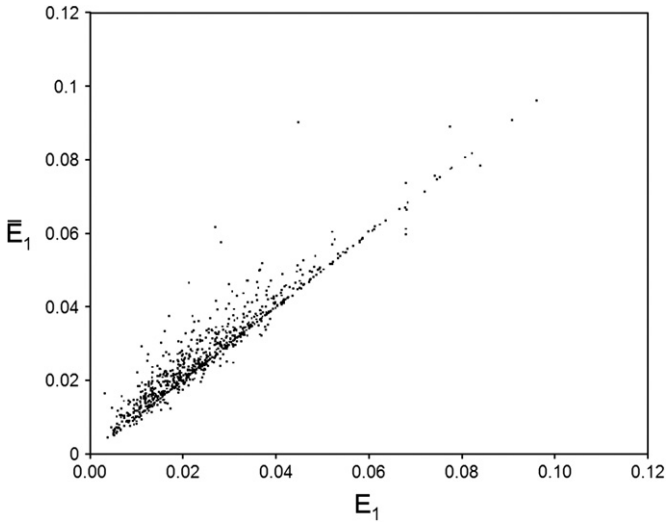


**Fig. 11.** The positive correlation between our two measures of efficiency. Each point represents one villus.

the top 5% of efficiencies) and low (bottom 5%) efficiency (as defined by $E_1$) villi (Table 3).

Clearly a hallmark of low efficiency is a large amount of capillaries 'crowded' into a villus—confirming that diffusional screening and system efficiency are related. As we previously stated, the current state of knowledge of the actual functional capacity of villi seen and diagnosed daily by surgical pathologists is such that whether these diagnosed capillary abnormalities cause or are merely correlated with the clinical outcomes linked to them (either fetal or maternal) is not known. The scope of future work involves several logical next steps. The current samples were confined to placentas delivered at term without diagnosed fetal growth restriction or maternal preeclampsia or diabetes. These authors are currently extending analyses to abnormal placentas, especially investigating what villous capillary geometries (and by

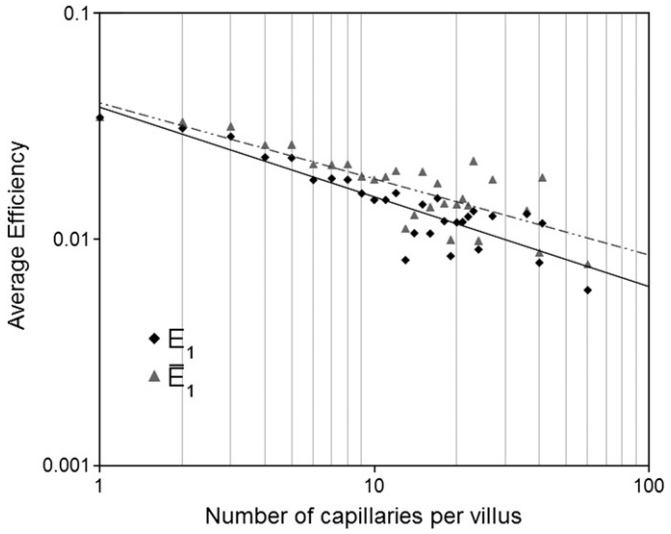


**Fig. 12.** Average $E_1$ and $\bar{E}_1$ as a function of number of capillaries per villus. The fitted lines correspond to power laws.

extension, functional efficiencies) are associated with and therefore may impact on—only maternal, only fetal and both maternal and fetal pathologies (Table 4).

## 4. Summary

A numerical simulation of diffusive transport in real villi combined with an automatic method of counting terminal villous geometry (areas, perimeters, etc.) is a novel way of quantifying oxygen transport in the placenta. We have used these techniques to measure the efficiency of various villous geometries. A number of different efficiencies were defined, with a common form of the ratio of oxygen flux to capillary area (proxies for 'revenue' and 'cost'). Every measure showed that villi containing many capillaries make up a large proportion of low-efficiency villi and that high efficiency villi almost exclusively only contain few capillaries. Our measures were correlated, and as a function of number of capillaries per villus followed power laws.

The notion of diffusional screening was introduced and potentially explains why large numbers of capillaries result in reduced efficiency. Central capillaries are often 'shielded' from oxygen and subsequently contribute little to the total oxygen flux of a villus. We have shown that intravillous diffusional screening leads to a measurable effect upon the oxygen uptake of the system. If oxygen fluxes calculated for isolated single capillaries (which we called isolated capillary flux) are compared with simulated oxygen fluxes, screening effects are easily highlighted. The screening factor, $\eta$, is our measure of how "shielded" a capillary is by other capillaries in the same villus. Capillaries experiencing no diffusional screening have $\eta = 1$, which decreases to zero for capillaries that are completely shielded from oxygen by other peripheral capillaries within a villus. It is believed that clinical complications that affect capillary vascular structure will lead to a measurable effect upon oxygen transport efficiency. The clinical effects of diffusion screening are to be investigated in future work.

In order for oxygen diffusion to be solved a number of assumptions have to be made that the concentration of oxygen at the villous membrane is constant for as long as it takes the diffusive system to relax and that all fetal capillaries act as perfect oxygen sinks. These assumptions were necessary to create an initial model, but future work aims to relax them. Although it is not possible from 2D slices to distinguish between capillaries

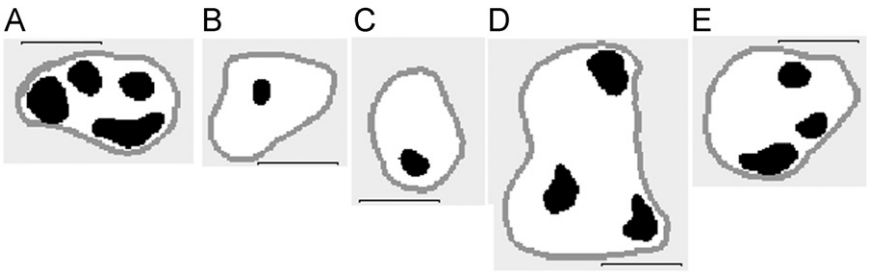


**Fig. 13.** Geometries of some high efficiency villi. The grey shaded area is the intervillous space, the darker grey line the villous membrane and the black areas fetal capillaries. The white area is the intravillous space, where diffusive oxygen transport is solved. The black scale line is 50 μm.

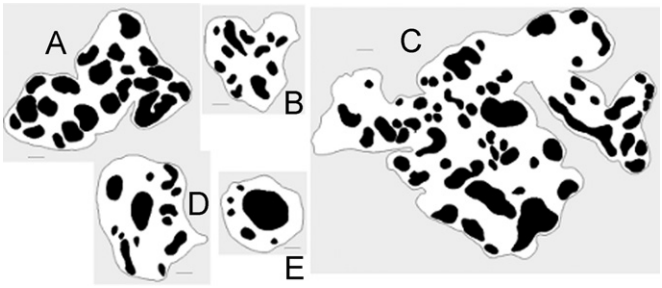


**Fig. 14.** Geometries of some low efficiency villi. The scale line is 50 μm.

**Table 3**
$E_1$ efficiencies for the capillaries in Fig. 13.

| Villus | $E_1$ | Harmonic mean boundary distance (μm) |
|---|---|---|
| A | 0.068 | 1.48 |
| B | 0.059 | 10.7 |
| C | 0.067 | 4.44 |
| D | 0.055 | 2.17 |
| E | 0.084 | 1.31 |

**Table 4**
$E_1$ efficiencies for the capillaries in Fig. 14.

| Villus | $E_1$ | Harmonic mean boundary distance (μm) |
|---|---|---|
| A | 0.0049 | 4.80 |
| B | 0.0069 | 6.20 |
| C | 0.0060 | 4.96 |
| D | 0.0056 | 6.54 |
| E | 0.0032 | 8.45 |

carrying oxygenated blood and those carrying blood to the sites of oxygen transfer, a further modification to our model could estimate this difference with a likely reduction in screening effects. Moreover, one may speculate that the screened central capillaries are likely to carry the already oxygenated blood back to the fetus. Such functional distinction between central and peripheral capillaries would significantly reduce the screening effect. Future medical investigations will hopefully clarify this important point.

There is scope for future work using the methods outlined in this paper: calculating the efficiency of various pathological placentas, finding distributions of villus and capillary sizes and shapes and the finding correlations between functional oxygen transport to clinical variables such as preeclampsia and maternal diabetes.

## Acknowledgements

The authors acknowledge valuable discussions with Dr. B. Sapoval and Dr. M. Filoche.

## Appendix A. Model of a circular villus with a single circular capillary

Conformal mapping allows the geometric transformation of a pair of non-concentric circles to a concentric pair. This simplifies oxygen flux calculations, allowing an analytical solution to be found. Let $L$ be the radius of the circle approximating the villus, $R$ the radius of the capillary, and $\delta$ the distance from the center of the capillary to the center of the villus (Fig. 15). The following conformal map describes how the region between two non-concentric circles, $z$, is transformed to a region between two concentric circles, $\omega$:

$$\omega = f(z) = \frac{az+bi}{ciz+d}, \tag{A.1}$$

where the coefficients $a$, $b$, $c$ and $d$ are given by:

$$a = Lr_0(L+\delta) - Rr_0^2,$$

$$b = L(r_0R^2 - r_0^2R - r_0\delta(L+\delta)),$$

$$c = r_0(L+\delta) - RL,$$

$$d = r_0\delta(L+\delta) - r_0R^2 + RL^2.$$

The radius of the transformed capillary $r_0$ can be written explicitly in terms of the parameters of the original model villus:

$$r_0 = \frac{L^2 - \delta^2 + R^2 - \sqrt{(L^2 - \delta^2 + R^2)^2 - 4R^2L^2}}{2R}. \tag{A.2}$$

Once $r_0$ is found, the equation for stationary diffusion can be solved within the region $z$ and the oxygen flux $J$ can be calculated as

$$J = \frac{2\pi D}{\ln(L/r_0)}. \tag{A.3}$$

Conformal mapping allows oxygen fluxes in a model villus to be quickly calculated. A villus containing one capillary should not experience any diffusion screening and so theoretical flux (A.3) should not differ from the calculated flux. Using Eq. (A.3) does not account for the presence of any other capillaries within a villus, and so will over-estimate the oxygen flux in these situations. For villi containing multiple capillaries, the amount that total theoretical flux differs from the calculated flux gives a quantitative measure of screening. A second screening factor $\chi$ is defined as the ratio of calculated and theoretical flux so that villi with $\chi = 1$ experience no screening.

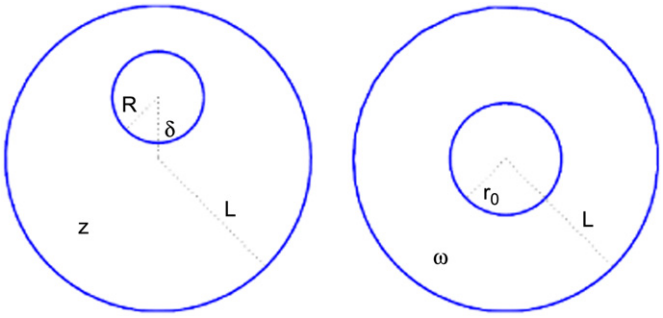


**Fig. 15.** A model villus of radius $L$ and a non-central capillary radius $R$ can be transformed to a concentric capillary of radius $r_0$. $\delta$ is the deviation from centrality and $z$ is the region of stationary diffusion. $\omega$ is the transformed region.

A number of assumptions need to be made in order to use conformal mapping real villi and capillaries have to be represented as non-concentric circles; this can be approximated by conserving their perimeters and shortest separation.

## References


Amer, H.Z., Heller, D.S., 2010. Chorangioma and related vascular lesions of the placenta–a review. Fetal Pediatr. Pathol. 29 (4), 199–206.

Barker, D.J.P., 1995. Fetal origins of coronary heart disease. Br. Med. J. 311, 171–174.

Benirschke, K., Kaufmann, P., Baergen, R., 2006a. Classification of villous maldevelopment. In: Pathology of the Human Placenta, 5th ed. Springer, New York.

Benirschke, K., Kauffmann, P., Baergen, R., 2006b. Table 28.1. In: The Pathology of the Human Placenta, 5th ed., Springer, New York.

Benirschke, K., Kaufmann, P., Baergen, R., 2006c. Architecture of normal villous trees. In: Pathology of the Human Placenta, 5th ed., Springer, New York, pp. 160–164 (Chapter 7).

Boyd, J.D., Hamilton, W.J. 1970. The utero-placental circulatory system. In: The Human Placenta. W Heffer and Sons Ltd, London.

Burton, G., Woods, A., Januiaux, E., Kingdom, J., 2009. Rheological and physiological consequences of conversion of the maternal spiral arteries for uteroplacental blood flow during human pregnancy. Placenta 30, 473–482.

Castellucci, M., Kaufmann, P., 1982. A three-dimensional study of the normal human placental villous core: II. Stromal architecture. Placenta 3 (3), 269–285.

Costa, A., Costantine, M.L., Fumero, R., 1992. Oxygen exchange mechanisms in the human placenta: mathematical modelling and simulation. J. Biomed. Eng. 14, 385–389.

Felici, M., Filoche, M., Sapoval, B., 2003. Diffusional screening in the human pulmonary acinus. J. Appl. Physiol. 94, 2010–2016.

Felici, M., Filoche, M., Straus, C., Similowski, T., Sapoval, B., 2005. Diffusional screening in real 3D human acini: a theoretical study. Respir. Physiol. Neurobiol. 145, 279.

Gill, J.S., Woods, M.P., Salafia, C.M., Vvedensky, D.D., 2011. Distributions functions for measures of placental shape and morphology, ArXiv:1109.2057.

Grebenkov, D.G., Filoche, M., Sapoval, B., Felici, M., 2005. Diffusion–reaction in branched structures: theory and application to the lung acinus. Phys. Rev. Lett. 94, 050602.

Hill, E., Power, G., Longo, L., 1973. A mathematical model of carbon dioxide transfer in the placenta and its interaction with oxygen. Am. J. Physiol. 224, 283–299.

Jaluria, Y., Torrance, K.E., 2002. Computational Heat Transfer, 2nd ed. Taylor & Francis, New York.

Kaufmann, P., Bruns, U., Leiser, R., Luckhardt, M., Winterhager, E., 1985. The fetal vascularisation of term human placental villi: II. Intermediate and terminal villi. Anat. Embryol. (Berl) 173 (2), 203–214.

Kirschbaym, T.H., Shapiro, N.Z., 1969. A mathematical model of placental oxygen transfer. J. Theor. Biol. 25, 380–402.

Lackman, F., Capewell, V., Gagnon, R., Richardson, B., 2001. Fetal umbilical cord oxygen values and birth to placental weight ratio in relation to size at birth. Am. J. Obstet. Gynecol. 185 (3), 674–682.

Lardner, T.J., 1975. A model for placental oxygen exchange. J. Biomech. 8, 1331–1334.

Lee, M.M., Yeh, M.N., 1983. Fetal circulation of the placenta: a comparative study of human and baboon placenta by scanning electron microscopy of vascular casts. Placenta 4 Spec. No. 515–526.

Lee, M.M., Yeh, M.N., 1986. Fetal microcirculation of abnormal human placenta: I. Scanning electron microscopy of placental vascular casts from small for gestational age fetus. Am. J. Obstet. Gynecol. 154 (5), 1133–1139.

Mayhew, T.M., Joy, C.F., Haas, J.D., 1984. Structure–function correlation in the human placenta: the morphometric diffusion capacity for oxygen at full term. J. Anat. 139 (4), 691–708.

Mayhew, T.M., Jackson, M.R., Haas, J.D., 1986. Microscopical morphology of the human placenta and its effects on oxygen diffusion: a morphometric model. Placenta 7, 121–131.

Mital, P., Hooja, N., Mehndiratta, K., 2002. Placental thickness: a sonographic parameter for estimating gestational age of the fetus. J. Radiol. Imag. 12 (4), 553–554.

Ogino, S., Redline, R.W., 2000. Villous capillary lesions of the placenta: distinctions between chorangioma chorangiomatosis and chorangiosis. Hum. Pathol. 31 (8), 945–954.

Salafia, C.M., Maas, E., Thorp, J.M., Eucker, B., Pezzullo, J.C., Savitz, D.A., 2005. Measures of placental growth in relation to birth weight and gestational age. Am. J. Epidemiol. 162 (10), 18.

Sen, D.K., Kaufmann, P., Schweikhart, G., 1979. Classification of human placental villi. II. Morphometry. Cell Tissue Res. 200 (3), 425–434.

Sood, R., Zehnder, J.L., Druzin, M.L., Brown, P.O., 2006. Gene expression patterns in human placenta. Proc. Natl. Acad. Sci. USA 103 (14), 5478–5483.

Weibel, E.R., 1970. Morphometric estimation of pulmonary diffusion capacity: I. Model and Method. Respir. Physiol. 11, 54–75.